Electronic Supplementary Information (ESI)

An RNase H-powered DNA walking machine for sensitive detection of RNase H and the screening of related inhibitors

Yafang Wang, Namin Hu, Chang Liu, Cunpeng Nie, Manman He, Juan Zhang, Qiaoqin Yu, Chuan Zhao, Tingting Chen* and Xia Chu*

State Key Laboratory of Chemo/Bio-Sensing and Chemometrics, College of Chemistry and Chemical Engineering, Hunan University, Changsha 410082, P. R. China

E-mail: xiachu@hnu.edu.cn; chenting1104@hnu.edu.cn

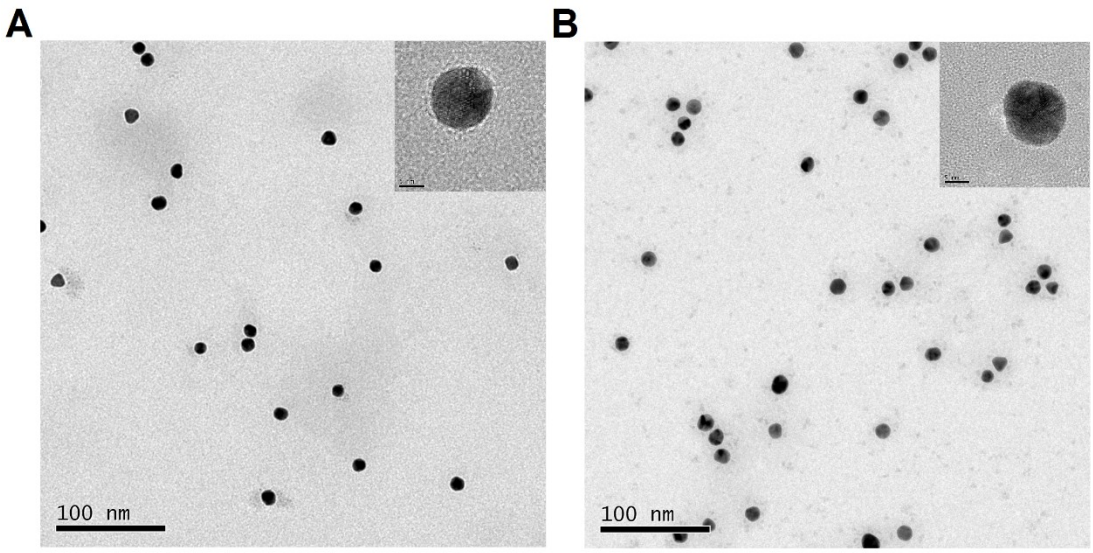

Fig. S1 Transmission electron microscopy images of the bare AuNPs (A) and the DNA-RNA chimeric strands functionalized AuNPs (B).

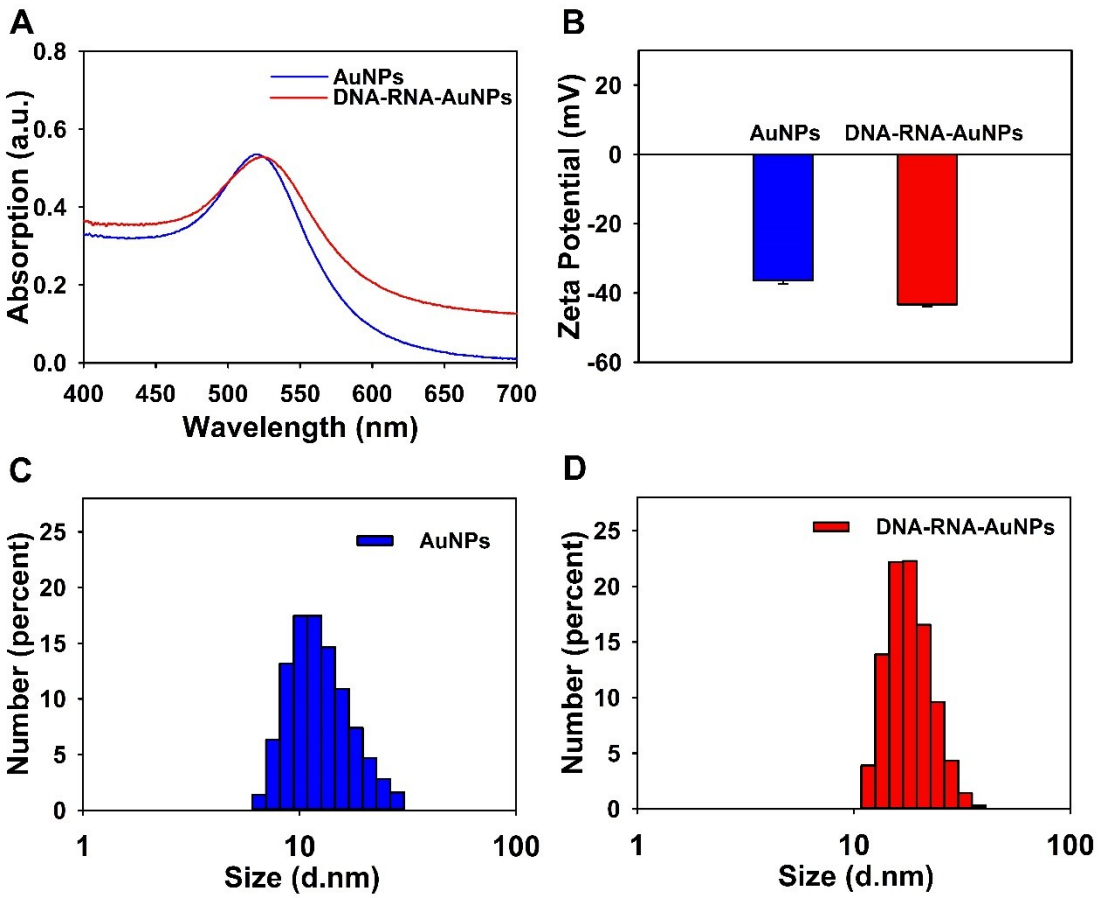

Fig. S2 (A) UV-vis absorption spectra of bare AuNPs (blue) and DNA-RNA chimeric strands functionalized AuNPs (red). (B) Zeta potential of bare AuNPs (blue) and DNA-RNA chimeric strands functionalized AuNPs (red). Dynamic light scattering (DLS) measurements of bare AuNPs (C) and DNA-RNA chimeric strands functionalized AuNPs (D).

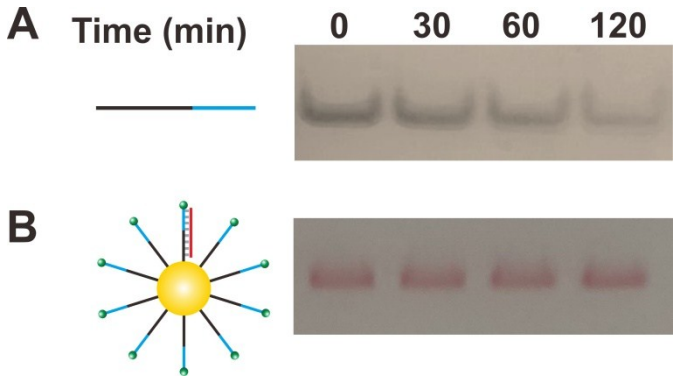

Fig. S3 Degradation analysis of the DNA-RNA chimeric strand (A) and DNA walking machine (B) against DNase I.

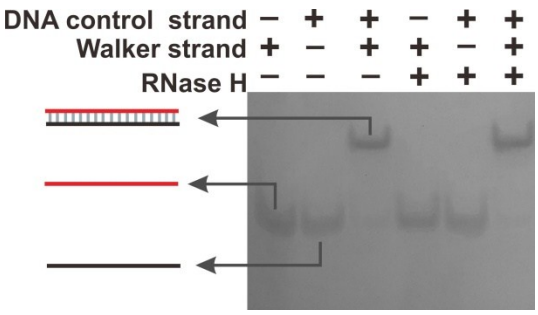

Fig. S4 Polyacrylamide gel electrophoresis image of DNA walker strand, DNA control strand and DNA hybrid strands in response to RNase H.

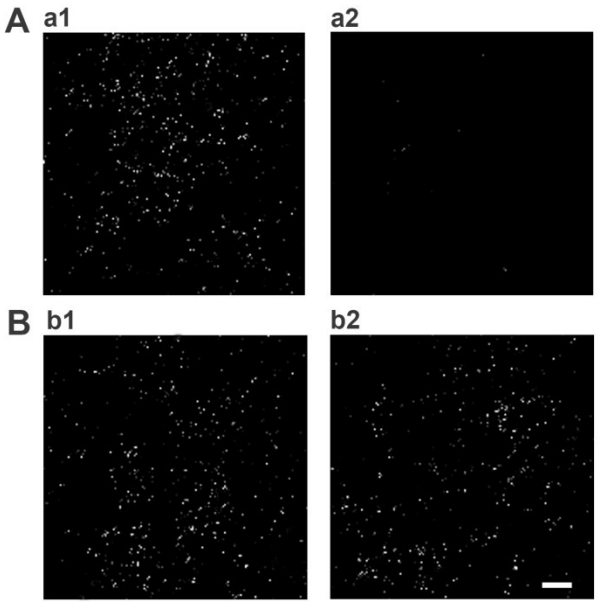

Fig. S5 TIRF images of different functionalized AuNPs. (A) The DNA walking machine in the absence (a1) or presence (a2) of RNase H. (B) The AuNPs conjugated with only DNA-RNA chimeric strands in the absence (b1) or presence (b2) of RNase H. Scale bar=3 μm.

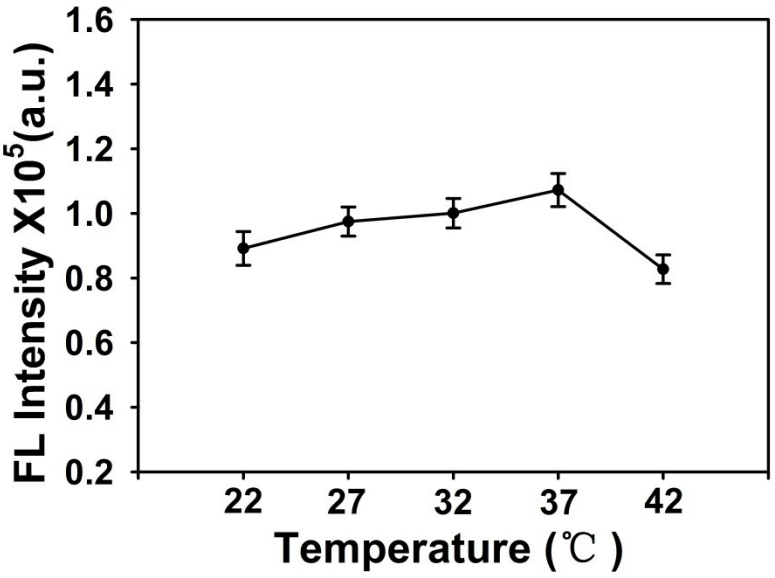

Fig. S6 Optimization experiment of temperature on the operation of DNA walking machine. Error bars were calculated from three replicate measurements.

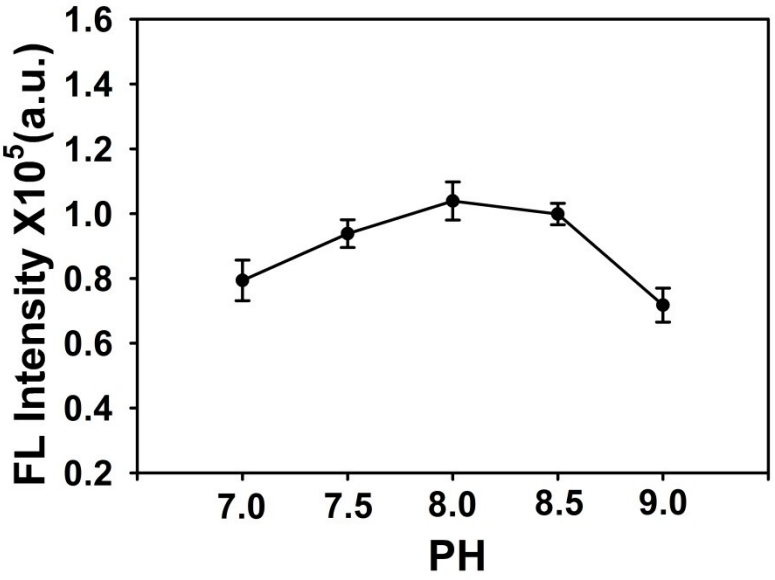

Fig. S7 Optimization experiment of pH on the operation of DNA walking machine. Error bars were calculated from three replicate measurements.

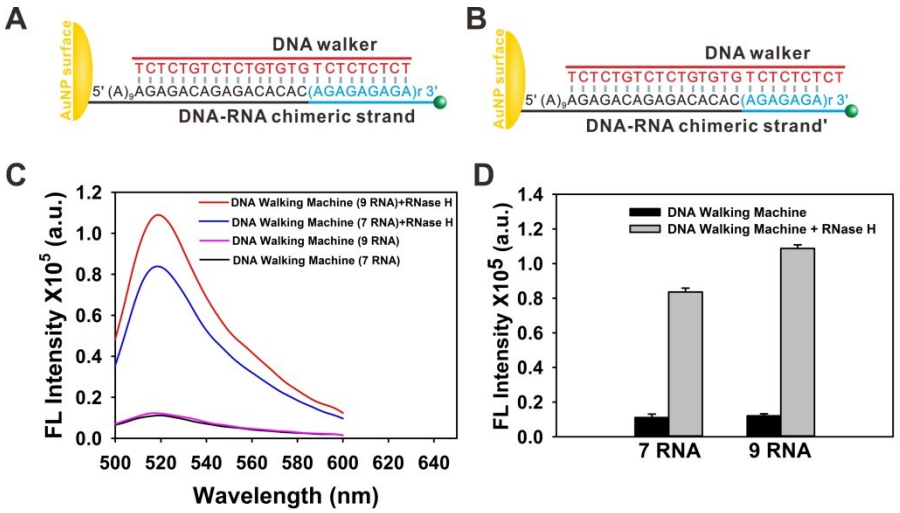

Fig. S8 (A) Construction of DNA-RNA chimeric strand (9 nt RNA). (B) Construction of DNA-RNA chimeric strand (7 nt RNA). (B) Fluorescence spectra of DNA walking machine constructed by DNA-RNA chimeric strand (9 nt RNA) and DNA-RNA chimeric strand (7 nt RNA) in response to RNase H. (C) Fluorescence intensities versus varying length of RNA in DNA-RNA chimeric strand.

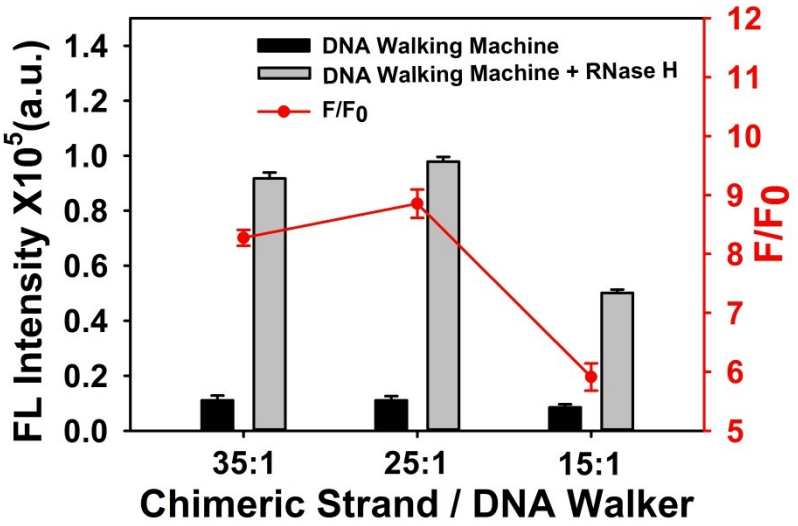

Fig. S9 Optimization experiment of the molar ratio of two strands on the operation of DNA walking machine. Error bars were calculated from three replicate measurements.

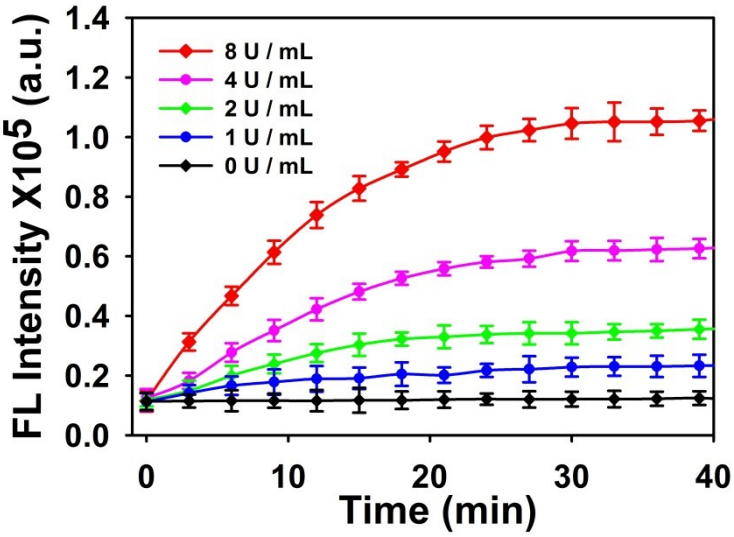

Fig. S10 Optimization experiment of reaction time on the operation of DNA walking machine. Error bars were calculated from three replicate measurements.

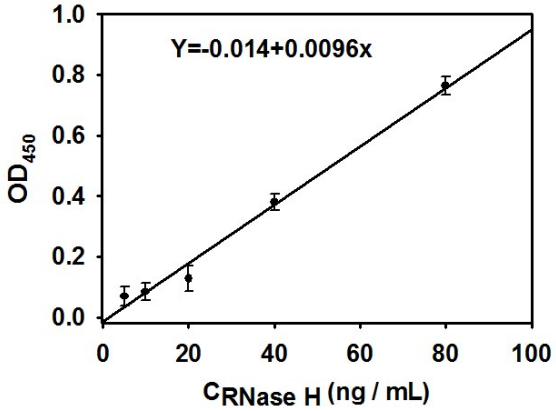

Fig. S11 The working curve of the RNase H standard sample by using commercial RNase H ELISA kit. Error bars were calculated from three replicate measurements.

Methods	Detection limit	Ref.
Gold nanoparticles	27 U / mL	1
Tb^{3+}-induced G-quadruplex conjugates	2 U / mL	2
DNA tetrahedron based biosensor	3.41 U / mL	3
N-methyl mesoporphyrin IX	0.2 U / mL	4
Iridium(III) complexes	0.125 U / mL	5

Table S1. Comparison of our analytical method with other reported methods for the detection of RNase H.

Sample number	OD_{450}	Mass concentration of RNase H (ng/mL)	Activity concentration of RNase H (U/mL)
1	0.238	26.25	1.05
2	0.227	25.10	1.00
3	0.223	24.69	0.99

1 unit of RNase H is 25 ng provided by the product manual.

Table S2. The detection results of the RNase H in 10% serum by using commercial RNase H ELISA kit. The concentration of the RNase H in 10% serum is 1.01±0.03 U/mL.

References

1. X. Xie, W. Xu, T. Li and X. Liu, *Small*, 2011, **7**, 1393-1396.
2. K. Wu, C. Ma, H. Liu, H. He, W. Zeng and K. Wang, *Anal. Methods*, 2017, **9**, 3055-3060.
3. K. Zhang, W. Huang, Y. Huang, H. Li, K. Wang, X. Zhu and M. Xie, *Anal. Chem.*, 2019, **91**, 7086-7096.
4. D. Hu, F. Pu, Z. Huang, J. Ren and X. Qu, *Chem. Eur. J.*, 2010, **16**, 2605-2610.
5. L. Lu, W. Wang, C. Yang, T.S. Kang, C.H. Leung and D.L. Ma, *J. Mater. Chem. B*, 2016, **4**, 6791-6796.